



ELSEVIER

τ -Al_{2.9}Ta_{2.7}V_{1.4}, a new type of pentagonal antiprismatic columnar structure

Bernd Harbrecht*, Norbert Rheindorf, Volker Wagner

Institut für Anorganische Chemie, Universität Bonn, Gerhard-Domagk-Straße 1, D-53121 Bonn, Germany

Received 5 May 1995; in final form 20 June 1995

Abstract

The so-called τ -phase occurring in the ternary system Al-Ta-V was prepared at 1273 K from bcc-Al_{35–48}Ta_{32–42}V_{17–30} solid solutions which themselves were obtained by arc-melting compressed mixtures of the elements. The structure of τ -Al_{2.9}Ta_{2.7}V_{1.4} was determined by means of X-ray powder diffractometry: $a = 509.94(2)$ pm; $b = 1198.69(5)$ pm; $c = 732.25(3)$ pm; space group, $Cmca$; $Z = 4$; Pearson symbol: oC28; $wR_p = 0.040$. The structure is made up of four crystallographically distinct metal atoms. Two sites are statistically occupied. All atoms have Frank–Kasper type coordination with 12, 15 and 16 nearest neighbours. The relative frequency of the distinct configurations is 3:2:2. τ -Al_{2.9}Ta_{2.7}V_{1.4} forms a new type of pentagonal antiprismatic columnar structure based on a tetrahedral close-packed arrangement of the atoms.

Keywords: Aluminium alloys; Crystal structure; Tetrahedral close-packed structure

1. Introduction

Recent preparative and structural reinvestigations of binary Al-Ta phases have uncovered three phases with triclinic, monoclinic and hexagonal symmetries, all with complicated structures [1,2], and Al₆₉Ta₃₉ [3], a new γ -brass-related giant cubic cell structure. In continuation of our efforts to unravel the phase relations in the binary and adjacent ternary systems we have studied the Al-Ta-V system in the neighbourhood of the so-called Y- [4] or τ -phase [5]. This phase was first found by Raman in 1966 [4] by generating an isotherm at 1273 K. Raman correctly located the phase around Al₄₀Ta₄₀V₂₀. The homogeneity range and the structure of the phase were not determined, however.

We studied the system prepared at 1073–2123 K in the compositional range Al_{28–55}Ta_{20–55}V_{10–35}. The electrical resistivity of selected samples was measured in the range 18–325 K. The structure of the τ -phase was solved by direct methods from integrated X-ray powder intensities and subsequently refined by fitting the diffraction profile. The results are reported here.

2. Experimental

2.1. Preparation

Al (99.93% Al, Eckart–Werke) was used as obtained. Ta (60 mesh, 99.8%, Ventron, Karlsruhe) and V (99.7%, Ventron) were inductively heated (Ta, 2173 K; V, 1773 K) in a tungsten crucible ($P < 10^{-3}$ Pa) prior to use. Compressed mixtures of the elements (approximately 500 mg per pellet, 48 samples) were arc-melted on a water-cooled copper plate under flowing Ar (3 l min⁻¹, 99.996% Ar, Messer Griesheim, Darmstadt) using a non-consumable tungsten tip as a second electrode. The composition was recalculated by subtracting the mass loss (<4 mg), assuming that only aluminium evaporates from the melt. The as cast samples were transferred into ampoules welded from tantalum tube (diameter 8 mm, Metallwerke Plansee Vertriebsgesellschaft, Ostfildern) under Ar. The ampoules were either sealed in previously evacuated quartz glass ampoules or heated under vacuum. The ingots were annealed at temperatures ranging from 1073 to 2123 K. The temperature was controlled using PtRh-thermocouples or a pyrometer depending on whether the samples were annealed in electrical resist-

* Corresponding author.

ance furnaces or in an induction furnace (h.f. generator HG 54, Himmelwerk, Tübingen). The accuracy of the specification of temperature is estimated to be $< \pm 30$ K.

2.2. X-Ray diffraction

All samples were characterised by X-ray diffraction using a Guinier camera FR552 (Enraf-Nonius, Delft, NL) and Cu-K α radiation. Highly pure silicon (from Heliotronic, $a = 543.10646(8)$ pm [6]) was used as an internal standard. Powder diffractograms (Cu-K α) were recorded at ambient temperature employing a diffractometer PW 1050/25 (Philips, Eindhoven, NL) driven by a controller UDS2 (Skoronek, Jülich). Intensities were measured every 0.03° for 60 s in the range $7^\circ \leq 2\theta \leq 100^\circ$. Data processing was accomplished using the program DIFFRAKT [7]. The crystal structure determination was performed by means of direct methods in combination with Fourier calculations using the program SHELX-76 [8]. The diffraction profiles were fitted by employing a modified Rietveld version [9]. The figures of the structure were drawn with SCHAKAL92 [10] and POLIEDRI [11], respectively.

2.3. Electron diffraction

Electron diffraction experiments were performed with a CM30ST microscope working at 300 kV (Philips, Eindhoven, NL). Vapour-deposited gold was used as the standard for the calculation of d spacings.

2.4. Electrical resistance

The electrical resistance of microcrystalline samples was measured in the temperature range 18–325 K using a heatable cold head D105 (Cryo Physics) connected to a closed-cycle He cryostat and a temperature controller (Lake Shore). Four copper wires were attached to pressed, sintered powder samples of $\text{Al}_{2.8}\text{Ta}_{2.8}\text{V}_{1.4}$, $\text{Al}_{2.9}\text{Ta}_{2.7}\text{V}_{1.4}$ and $\text{Al}_{3.1}\text{Ta}_{2.5}\text{V}_{1.4}$ with

silver paste. The outer wires were connected to a dc current generator TR 6142 (Advantest). The decay of voltage at constant current was measured between the two inner contacts every five degrees. The large internal resistance of the digital multimeter 195 A (Keithley) guaranteed the elimination of contact resistance. Thermopower effects were compensated by switching the current flow.

3. Results and discussion

3.1. Homogeneity range and phase relations

As cast bcc solid solutions of compositional range $\text{Al}_{35-48}\text{Ta}_{32-42}\text{V}_{17-30}$ transform in a solid state reaction below 1473 K into the τ -phase. Samples richer in aluminium and poorer in tantalum contain phases of the $\text{Al}_{69}\text{Ta}_{39}$ -type [3] and the Al_3Ta -type [12] as by-products. The σ -phase [13] is present in samples richer in tantalum. A conclusive indexation of a Guinier diagram of the τ -phase on the basis of a C-centred orthorhombic lattice was obtained by applying the indexing routine TREOR [14].

A noticeable phase width is indicated by a variation of the lattice parameters: a , 505.1–510.9 pm; b , 1197.5–1202.7 pm; c , 720.2–733.9 pm; (see Table 1). The values of the a and c axes particularly depend on the metal ratios V/Ta and Al/Ta respectively.

Along with the diffraction patterns of the τ -phase between four and ten extra reflections of very weak intensity were always observed. The four reflections of highest intensity are marked by arrows in Fig. 1. Contamination by oxygen was excluded as cause for the additional reflections: synthesis in the presence of 0.5 mol% oxygen added in form of Ta_2O_5 did not lead to an increase in the intensities of the extra reflections. However, the formation of a superstructure associated with possible ordering of atoms on two statistically occupied sites was ruled out by electron diffraction experiments which proved the translational symmetries

Table 1
Lattice parameters of the τ -phase depending on composition of the samples; coexisting phases

Composition	a (pm)	b (pm)	c (pm)	R_1^a	Coexisting phases
$\text{Al}_{30}\text{Ta}_{35}\text{V}_{35}$	508.0(3)	1202.7(4)	732.2(3)	—	σ -type
$\text{Al}_{55}\text{Ta}_{25}\text{V}_{20}$	510.9(8)	1200.4(8)	720.2(3)	—	$\text{Al}_{69}\text{Ta}_{39}$ -type
$\text{Al}_{45}\text{Ta}_{25}\text{V}_{25}$	505.1(1)	1197.5(2)	725.7(2)	—	Al_3Ta -type
$\text{Al}_{35}\text{Ta}_{35}\text{V}_{30}$	506.57(2)	1199.20(6)	732.21(3)	0.0397	$\text{Al}_{69}\text{Ta}_{39}$ -type
$\text{Al}_{46}\text{Ta}_{36}\text{V}_{18}$	510.47(3)	1197.90(7)	733.94(4)	0.0437	—
$\text{Al}_{45}\text{Ta}_{35}\text{V}_{20}$	509.94(2)	1198.69(5)	732.25(3)	0.0146	—

^a Residual value $R_1 = \sum |I_{\text{obs}} - I_{\text{calc}}| / \sum I_{\text{obs}}$ of the profile refinement; if no R -value is stated, the lattice parameters were calculated from Guinier data.

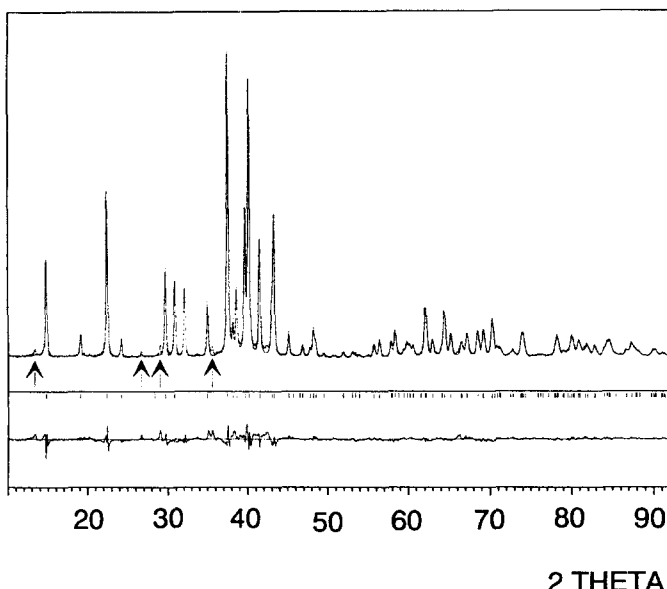


Fig. 1. Measured and calculated X-ray powder diffractogram of τ -Al₄₅Ta₃₅V₂₀; the difference plot is shown in the lower part of the figure. Arrows indicate the locations of the four strongest reflections of an unknown by-product.

to be correct. A conclusive indexation of these reflections was not found. Their origin remains obscure for the present.

3.2. Structure determination

Owing to the groups of systematically extinct reflections the symmetry of the structure was assumed to be *Cmca*. Taking this space group as a basis the structure could be solved from integrated intensities (program DIFFRAKT [7]) by direct methods (Ta) in combination with Fourier syntheses (V, Al). Subsequent diffraction profile fitting [9] converged at $R_1 = 0.0146$, $R_p = 0.0270$ and $wR_p = 0.0400$. These results were obtained with the assumptions that (i) all sites were completely occupied and (ii) all three distinct metal atoms do not occupy a single site. In view of the existence of the bcc solid solution the latter assumption does not always hold. However, this constraint is necessary for an unambiguous refinement of the site occupancy factors. The metals assigned to the electron density were chosen with consideration of the composition of the samples.

Fig. 1 shows the profile fit together with the difference plot of a sample of composition Al₄₅Ta₃₅V₂₀. Intensities and *hkl* values of reflections with $2\theta < 50^\circ$ are listed in Table 2. Table 3 gives essential information concerning the profile fitting. Positional and displacement parameters are listed in Table 4, relevant interatomic distances are listed in Table 5.

Table 2
Indexation of τ -Al₄₅Ta₃₅V₂₀, 2θ -values ($<50^\circ$, Cu-K α_1), observed and calculated intensities

<i>h</i>	<i>k</i>	<i>l</i>	2θ	<i>I</i> _{calc}	<i>I</i> _{obs}
0	2	0	14.768	295	286
0	2	1	19.119	64	64
1	1	1	22.485	497	494
0	0	2	24.289	54	52
0	2	2	28.544	1	1
0	4	0	29.788	265	267
1	3	1	30.917	13	12
1	1	2	30.953	222	217
0	4	1	32.249	216	212
2	0	0	35.167	162	170
1	3	2	37.672	999	1000
2	2	0	38.330	83	87
0	4	2	38.799	210	216
0	2	3	39.843	476	487
2	2	1	40.331	932	943
1	1	3	41.674	410	413
2	0	2	43.201	139	136
1	5	1	43.466	482	473
0	6	0	45.355	79	82
2	2	2	45.899	1	1
2	4	0	46.737	4	4
1	3	3	47.088	1	1
0	6	1	47.111	41	40
0	4	3	48.033	25	25
2	4	1	48.454	92	94
1	5	2	48.746	42	43
0	0	4	49.765	4	13

Table 3
Parameters of the Rietveld refinement of Al_{2.9}Ta_{2.7}V_{1.4}

Nominal composition	Al ₄₅ Ta ₃₅ V ₂₀
Composition according to Rietveld	Al ₄₁ Ta ₃₈ V ₂₁
Parameters	
Range (2θ) ($^\circ$) step width ($^\circ$)	10-95/0.03
Count time per step (s)	60
Radiation	Cu-K α
Refined phases	1
Number of variables	25
Profile fit	pseudo-Voigt
Background	refined
Structure and profile data	
Molar mass (g mol ⁻¹)	653.5
Space group	<i>Cmca</i> (64)
Lattice parameters <i>a</i> (pm)	509.94(2)
<i>b</i> (pm)	1198.69(5)
<i>c</i> (pm)	732.25(3)
Volume (10 ⁶ pm ³)	447.59(3)
Number of formula units <i>Z</i>	4
Halfwidth parameters <i>U</i>	0.27(2)
<i>V</i>	-0.14(1)
<i>W</i>	0.056(2)
Asymmetry parameter	0.16(2)
Peak shape parameter γ	0.79(1)
<i>R</i> -values	
<i>R</i> ₁	0.0146
<i>R</i> _p	0.0270
<i>wR</i> _p	0.0400

Table 4

Atomic coordinates and equivalent isotropic displacement parameters of $\text{Al}_{2.9}\text{Ta}_{2.7}\text{V}_{1.4}$

Atom	Site	<i>x</i>	<i>y</i>	<i>z</i>	<i>B</i> (10^4 pm^2)
Ta1	8f	0	0.4122(1)	0.1292(2)	1.75(5)
V1/Ta2 ^a	8e	0.25	0.6297(2)	0.25	1.7(1)
Al1/Ta3 ^b	4a	0	0	0	0.8(2)
Al2	8f	0	0.2858(6)	0.4362(11)	1.0(2)

^a Site occupancy factor $f_{\text{V}1} = 1 - f_{\text{Ta}2} = 0.73(1)$.

^b $f_{\text{Al}1} = 1 - f_{\text{Ta}3} = 0.88(1)$.

Table 5

Interatomic distances (pm) for $\text{Al}_{2.9}\text{Ta}_{2.7}\text{V}_{1.4}$

Ta1	Al2	1 \times 271.1(8) 1 \times 276.0(8) 2 \times 300.6(4)	Al1	Al2	2 \times 261.5(8) V1
				Ta1	2 \times 291.3(1)
Ta1		1 \times 283.1(2) 2 \times 310.4(1)			4 \times 291.6(1)
Al1		1 \times 291.3(1) 2 \times 291.6(1)	Al2	Al1	1 \times 261.5(8)
V1		2 \times 303.6(2) 2 \times 309.6(1) 2 \times 372.3(1)		V1	2 \times 263.7(7)
V1	V1	2 \times 255.0(0)		V1	2 \times 282.0(7)
Al2		2 \times 263.7(7) 2 \times 282.0(7)		Ta1	1 \times 271.1(8)
Al1		2 \times 272.0(1)			1 \times 276.0(8)
Ta1		2 \times 303.6(2) 2 \times 309.6(1)			2 \times 300.6(4)

3.3. Features of the crystal structure

A projection of the structure of $\tau\text{-Al}_{2.9}\text{Ta}_{2.7}\text{V}_{1.4}$ along *a* is shown in Fig. 2(a). The structure is composed of four crystallographically distinct atoms located in mirror planes perpendicular to *a* at heights *x* = 0, 1/2 (Ta1, Al1/Ta3 and Al2) or in glide planes at heights *x* and *z* = 1/4, 3/4 (V1/Ta2). Two sites, Al1/Ta3 and V1/Ta2, are statistically occupied. The atoms in the mirror planes are arranged in irregular primary nets. As may be clearly seen in Fig. 2(b), there are three distinct vertex configurations [15]: 5353 (Al1), 3²535 (Al2), and 3²5² (Ta1). Such vertex configurations necessarily imply irregular triangles and pentangles. Neighbouring nets are shifted according to the centring of the lattice, thus forming edge- and face-shared (parallel e.g. [0 1 -1] and [0 1 1]) pentagonal antiprismatic columns which have V1/Ta2 in the centre. Fig. 3 emphasises this feature of the structure. Interestingly, the condensation and orientation of the antiprismatic columns are highly specific in so far as the space in between them is completely filled by distorted metal tetrahedra. The three distinct tetrahedra, Al2₃Ta₁, Al1Al2Ta1₂ and Al2₂Ta1₂, are arranged in chains consisting of *trans*-edge-sharing stellae quadrangulæ, i.e. four tetrahedra fused via a fifth central one. Since the centred pentagonal antiprism

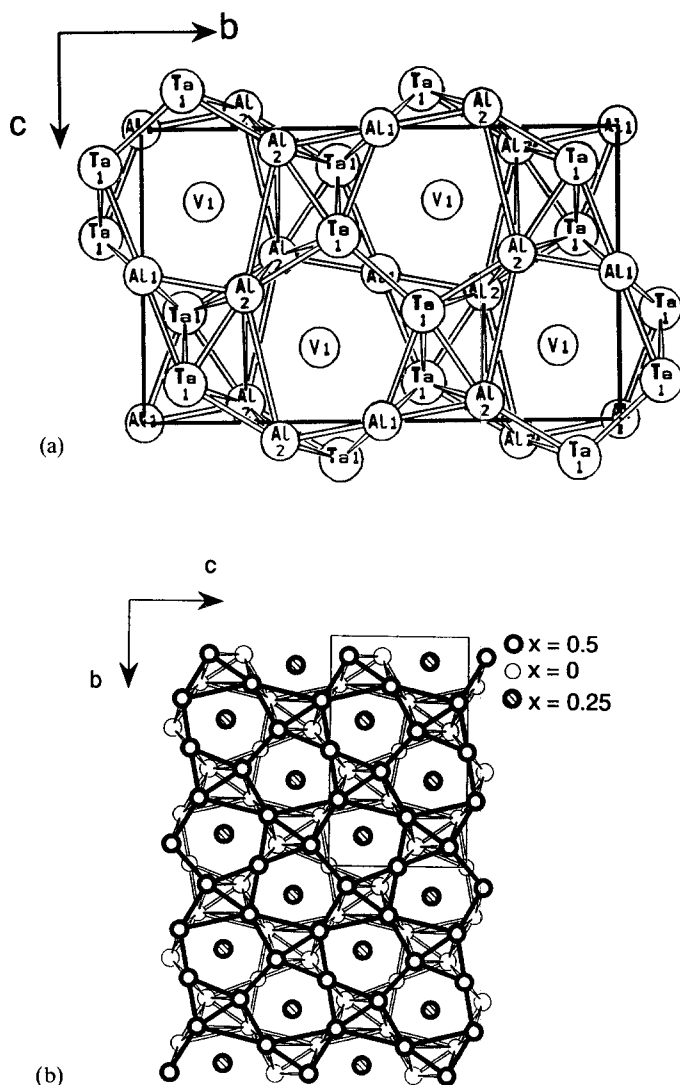


Fig. 2. The structure of $\tau\text{-Al}_{2.9}\text{Ta}_{2.7}\text{V}_{1.4}$ (a) viewed along the *a* axis; (b) with emphasis on the irregular nets formed by Al1, Al2 and Ta1.

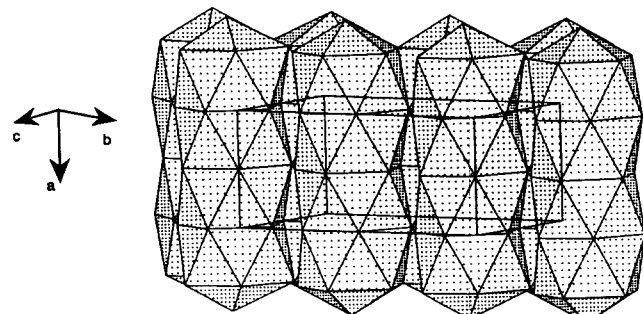


Fig. 3. View of the structure of $\tau\text{-Al}_{2.9}\text{Ta}_{2.7}\text{V}_{1.4}$ with emphasis on the arrangement of highly condensed columns running parallel to *a*.

matic columns can also be subdivided in tetrahedra, the structure can be considered as a specific tetrahedral close-packed arrangement. With respect to this feature the structure is unique among those comprised of pentagonal antiprismatic columns, such as Al_5Fe_2

[16], or distinct modifications of tantalum-rich sulphides such as Ta_6S [17,18] or $Ta_{6-x}V_xS$ [19]. In none of these pentagonal antiprismatic columnar structures is the volume between the columns so small: the degree of condensation of pentagonal antiprismatic columns reaches its maximum in the structure of the τ -phase.

The characteristic features of a tetrahedral close-packed (tcp) structure are reflected in the local coordination configurations, all of which are of the Frank-Kasper type [20,21] (see Fig. 4). The coordination numbers CN { } and mean distances $\langle \rangle$ are for Al1 {12}, $\langle 280.0 \text{ pm} \rangle$, for V1 {12}, $\langle 281.0 \text{ pm} \rangle$, for Al2 {15}, $\langle 304.5 \text{ pm} \rangle$, and for Ta1: {16}, $\langle 306.1 \text{ pm} \rangle$. As is indicated by the range of distances in the primary coordination sphere (Table 5), all polyhedra except for that about Al1 are significantly distorted. Nevertheless, they interpenetrate completely, as is typical for tcp structures [20-23]. The degree of distortion results from the frequency of the three distinct coordination configurations, 3{12}:2{15}:2{16}. This frequency corresponds to an average CN of 14.0 compared to 13.33-13.50 for Frank-Kasper phases [20,21]. This mean value is too large for a tcp structure fulfilling the requirements of the dihedral angle principle [23]. This states that the mean dihedral angle of all distorted tetrahedra in tcp structures does not differ by more than 0.1° from the dihedral angle of a tetrahedron, i.e. $\cos^{-1}(1/3)$.

The τ -phase is a moderate metallic conductor with a resistivity in the $\text{m}\Omega \text{ cm}$ range (see Fig. 5). Finally, it should be mentioned that we decided to retain the label τ [5] in order to emphasise the relationship between this structure type and that of σ -phases. Note

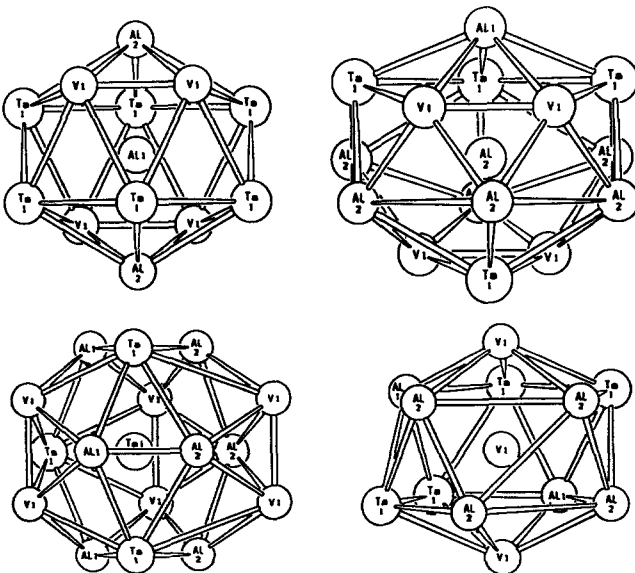


Fig. 4. Coordination polyhedra around the four crystallographically distinct atoms.

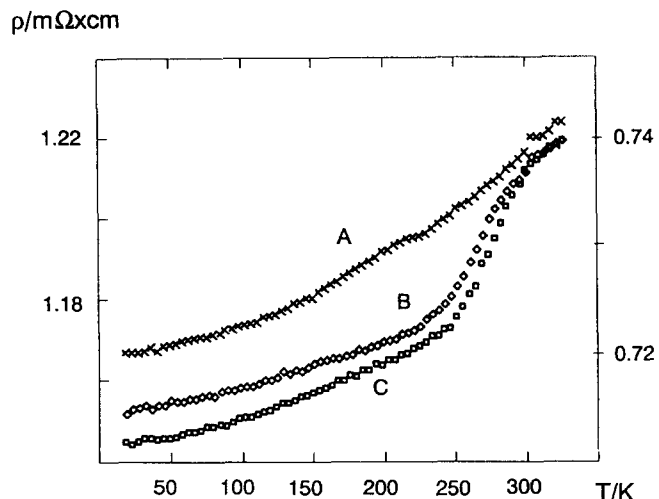


Fig. 5. Temperature dependence of the specific electrical resistivity of three τ -phases: (A) $Al_{42}Ta_{38}V_{20}$; (B) $Al_{43}Ta_{36}V_{21}$ (lefthand scale); (C) $Al_{44}Ta_{36}V_{20}$ (righthand scale).

that a σ -type phase exists in the neighbourhood of the τ -phase (see Table 1).

4. Conclusions

(i) The τ -phase occurring in the ternary system $Al-Ta-V$ forms at 1273 K from bcc- $Al_{35-48}Ta_{32-42}V_{17-30}$ solid solutions in a solid-state reaction.

(ii) The structure of the τ -phase represents a new type of a pentagonal antiprismatic columnar structure. The specific condensation and orientation of the columnar units afford a unique tetrahedral close-packed structure.

Acknowledgements

We thank Dr. F. Krumeich for performing the electron diffraction experiments. Financial support by the Fonds der Chemischen Industrie is gratefully acknowledged.

References

- [1] S. Mahne, F. Krumeich and B. Harbrecht, *J. Alloys Comp.*, 201 (1993) 167.
- [2] S. Mahne, B. Harbrecht and F. Krumeich, *J. Alloys Comp.*, 218 (1995) 177.
- [3] S. Mahne and B. Harbrecht, *J. Alloys Comp.*, 203 (1994) 271.
- [4] A. Raman, *Z. Metallkd.*, 57 (1966) 535.
- [5] G. Petzow and G. Effenberg (eds.), *Ternary Alloys: A Comprehensive Compendium of Evaluated Constitutional Data and Phase Diagrams*, VCH, Weinheim, 1993.
- [6] R.D. Deslattes, A. Henins, *Phys. Rev. Lett.*, 36 (1976) 898

- [7] V. Wagner and Th. Degen, DIFFRAKT, a PASCAL program for processing of powder data, University of Bonn, 1994.
- [8] G. Sheldrick, SHELX-76, program for crystal structure determination, University of Cambridge, 1976.
- [9] C.J. Howard and R.J. Hill, LHPM 7, Rietveld analysis program, AAEC Rep. No. M112, 1986.
- [10] E. Keller, SCHAKAL, a FORTRAN program for the graphic representation of molecular and crystallographic models, University of Freiburg, 1992.
- [11] T. Pilati, POLIEDRI, a FORTRAN program designed for plotting any kind of convex polyhedron, XVth congress of the International Union of Crystallography, Bordeaux, Collected Abstracts, 1990, C-69.
- [12] G. Brauer, Z. Anorg. Allg. Chem., 242 (1939) 1.
- [13] L.E. Edshammar and B. Holmberg, Acta Chem. Scand., 14 (1960) 1219.
- [14] P.E. Werner, TREOR, trial and error program for indexing of unknown powder patterns, University of Stockholm, 1988.
- [15] H.M. Cundy, A.P. Rollet, *Mathematical Models*, Clarendon Press, Oxford, 1952, p. 56.
- [16] U. Burkhardt, Yu. Grin and M. Ellner, Acta Crystallogr., B50 (1994) 313.
- [17] H.F. Franzen and J.G. Smegall, Acta Crystallogr., B26 (1970) 125.
- [18] B. Harbrecht, J. Less-Common Met., 138 (1988) 225.
- [19] B. Harbrecht and H.F. Franzen, Z. Anorg. Allg. Chem., 551 (1987) 74.
- [20] F.C. Frank and J.S. Kasper, Acta Crystallogr., 11 (1958) 184.
- [21] F.C. Frank and J.S. Kasper, Acta Crystallogr., 12 (1959) 483.
- [22] P.I. Kripyakevich and Ya.P. Yarmolyuk, Kristallografiya, 19 (1974) 539.
- [23] D.P. Shoemaker and C.B. Shoemaker, Acta Crystallogr., B42 (1986) 3.